ELSEVIER

Journal of Alloys and Compounds 293–295 (1999) 150–155

Journal of ALLOYS AND COMPOUNDS

The intrinsic degradation behavior of $(V_{0.53}Ti_{0.47})_{0.925}Fe_{0.075}$ alloy during temperature-induced hydrogen absorption-desorption cycling

Jeoung-Gun Park*, Dong-Myung Kim, Kuk-Jin Jang, Jai-Sung Han, Kurn Cho, Jai-Young Lee

Department of Materials Science and Engineering, Korea Advanced Institute of Science and Technology, 373-1 Kusong-dong, Yusong-gu, Taejon, South Korea

Abstract

The intrinsic degradation behavior of an $(V_{0.53}Ti_{0.47})_{0.925}Fe_{0.075}$ alloy having a BCC structure and two plateau regions (the low and high plateau region) has been investigated using P–C isotherm measurements, thermal desorption analysis, XRD and TEM analysis during temperature-induced hydrogen absorption–desorption cycling (thermal cycling). After 400 thermal cycles between room temperature and 600°C under 10 atm H_2, the total reversible hydrogen absorption capacity decreases by about 40%. In the low plateau region the reversible hydrogen absorption capacity decreases by about 24% after 400 cycles. The majority of the capacity loss takes place during the first 243 cycles. In the high plateau region, however the reversible hydrogen absorption capacity decreases by about 16% gradually with cycling. From the result of the thermal desorption analysis, it is found that the peak obtained at high temperature corresponds to the desorption of hydrogen of the low plateau region which shifts to lower temperatures and the peak area decreases after 223 cycles and then the area is maintained without any clear change up to 400 cycles. The low temperature peak corresponds to desorption of hydrogen from the high plateau; this does not shift but its peak area decreases gradually with cycles. From P–C isotherm measurements it is also found that the degradation behavior at each plateau region is different. In addition, XRD analysis shows that the crystal structure of the de-hydrided sample changes from BCC to BCT after degradation; the hydrided sample maintains FCC structure although the peaks are broadened after degradation. From the result of a static isothermal hydrogenation treatment, it is found that the change of crystal structure from BCC to BCT is caused only by temperature effects. The result of TEM analysis shows that peak broadening is caused by the formation of an amorphous phase in the FCC matrix.

Keywords: Thermal cycling; Plateau region; Degradation; Phase transformation; Amorphous

1. Introduction

In recent years, much attention has been paid to metal hydrides for application in thermal energy conversion systems such as heat pump and steam regeneration plants [1–5]. In such applications, one of the most important factors to be considered is the intrinsic degradation behavior such as the deterioration of the hydrogenation properties of alloys by hydrogen absorption–desorption cycling. Many of studies of metal hydride systems have been carried out to investigate the intrinsic degradation behavior and corresponding mechanisms [6–12].

It was reported that many BCC solid solution alloys were promising candidate materials because of their high hydrogen storage capacity of about 3~4 wt% and large hydride formation enthalpy [13]. In particular, $(V_{0.53}Ti_{0.47})_{0.925}Fe_{0.075}$ alloy has many advantages such as easy activation and fast hydrogen desorption [13]. However, this alloy has two plateau regions, a high and low pressure plateau region, respectively. The plateau pressure of the low plateau region is very low at room temperature so that the total hydrogen storage capacity of both the high and low plateau regions cannot generally be used. In addition, the plateau pressure increase as the temperature of alloy increases. The low plateau region can increase to the ambient pressure at high temperatures and the total stored hydrogen in the alloy can then be used. This alloy is therefore very promising in applications for thermal energy conversion systems operated at high temperature. There has been no experimental reports on the intrinsic degradation behavior of this alloy. In this study, the degradation behavior of the $(V_{0.53}Ti_{0.47})_{0.925}Fe_{0.075}$ BCC solid solution alloy was investigated before and after thermal cycling at high temperature

---

*Corresponding author.

0925-8388/99/$ – see front matter
PII: S0925-8388(99)00383-7

2. Experimental details

The $(V_{0.53}Ti_{0.47})_{0.925}Fe_{0.075}$ BCC solid solution alloy sample was prepared by arc melting under an argon atmosphere. To ensure homogeneity, it was remelted four times. The as-received alloy was confirmed by XRD to be a homogeneous single BCC solid solution phase. The alloy was mechanically crushed into powder (100~200 mesh) in air. Powder samples of about 1 g were employed for *P–C* isotherm measurements. *P–C* isotherm measurements, static isothermal hydrogenation treatment, and thermal desorption analysis were carried out in an automatic Sievert-type apparatus described elsewhere [14]. The samples were activated by heat treatment at 600°C for 30 min under a hydrogen pressure of 40 atm. Thermal cycling from room temperature to 600°C was performed on the activated samples with a 20 min cycle time under a charging pressure of 40 atm H_2. In order to observe the degradation behavior in the aspect of hydrogen storage capacity, the *P–C* isotherm measurements were carried out at several temperatures before and after thermal cycling. The thermal desorption analysis was performed on samples in both activated and degraded states. For the thermal desorption analysis, each sample was first fully hydrided under a hydrogen pressure of 40 atm at room temperature and then heated at a uniform heating rate of 5 K/min. The amount of evolved hydrogen was measured. The evolution rate was defined as the amount of desorbed hydrogen during the pressure change from 0.05 to 0.5 atm in unit time; it was plotted against temperature. This alloy had three phases, α solid solution phase, β, and γ hydride phase. To observe the change of structure after degradation it was necessary to obtain XRD data for both samples in de-hydrided and hydrided state before and after cycling respectively. To de-hydride the sample, it was heated at 600°C in vacuum. The α phase remained unchanged after this treatment since the α phase is very stable. To maintain the sample in a hydrided state, the sample was fully hydrogenated under a hydrogen charging pressure of 40 atm. The sample was quenched in cold water and then exposed to dry air. A static isothermal hydrogenation treatment at high temperature was performed to verify the effect of thermal energy during thermal cycling. In this experiment, the activated sample in the reactor was heat treated at 600°C for 48 h under a charging pressure of 40 atm H_2. Its microstructure was investigated using TEM. The TEM specimen was prepared by crushing the degraded sample in acetone.

3. Results and discussion

Generally the *P–C* isotherm is composed of the solid solution regions of α and β phase, and the region of two phases coexisting $\alpha+\beta$ phase (plateau region). The degradation behavior is well defined only at plateau region in the *P–C* isotherms. V–Ti based alloys are known to have two plateau regions, namely the one plateau region of $\alpha+\beta$ phase and the other of $\beta+\gamma$ phase. Because α phase is more stable than γ phase, the plateau pressure of $\alpha+\beta$ phase region is lower than that of $\beta+\gamma$ phase region and the plateau region of $\alpha+\beta$ phase is called a low plateau region and the plateau region of $\beta+\gamma$ phase a high plateau region.

To observe the degradation behavior of $(V_{0.53}Ti_{0.47})_{0.925}Fe_{0.075}$ it is necessary to measure *P–C* isotherms at several temperatures for each plateau region. Fig. 1 shows the *P–C* isotherms obtained before cycling at several temperatures. The high and low plateau regions are well observed at 150 and 600°C respectively. The total hydrogen storage capacity composed of each capacity of low and high plateau regions is about 2 H/M (4 wt%). This hydrogen storage capacity represents the amount of hydrogen absorbed at a hydrogen pressure of 40 atm. After *P–C* isotherm measurements at several temperatures to establish the hydrogen storage capacity and pressure of the plateau region for the as-received sample, thermal cycling was initiated on this sample to determine the extent of degradation. Fig. 2(a) and (b) show the *P–C* isotherms of $(V_{0.53}Ti_{0.47})_{0.925}Fe_{0.075}$ alloy after thermal cycles 24, 243, and 400 at two different plateau regions. Fig. 2(a) shows *P–C* isotherms for the low plateau region after several cycles. The hydrogen storage capacity decreases by about 24% after 400 cycles, but the major capacity loss takes place during the initial 243 cycles. Fig. 2(b) shows the *P–C* isotherms only including the high plateau region after several cycles. The total hydrogen storage capacity obtain

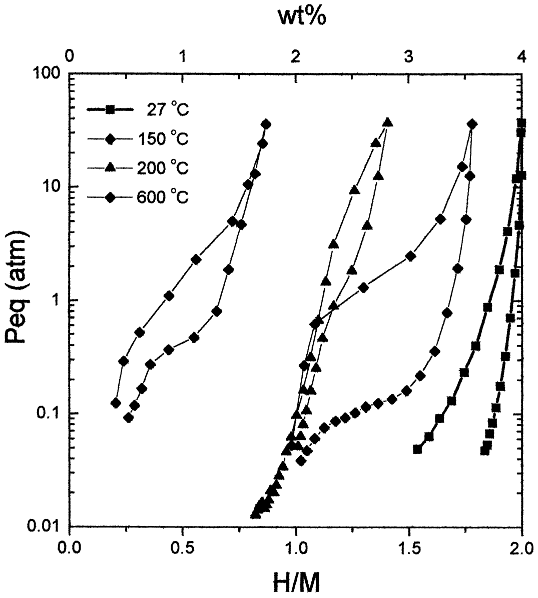

Fig. 1. *P–C* isotherms of $(V_{0.53}Ti_{0.47})_{0.925}Fe_{0.075}$ at several temperatures 30, 150, 200, and 600°C.

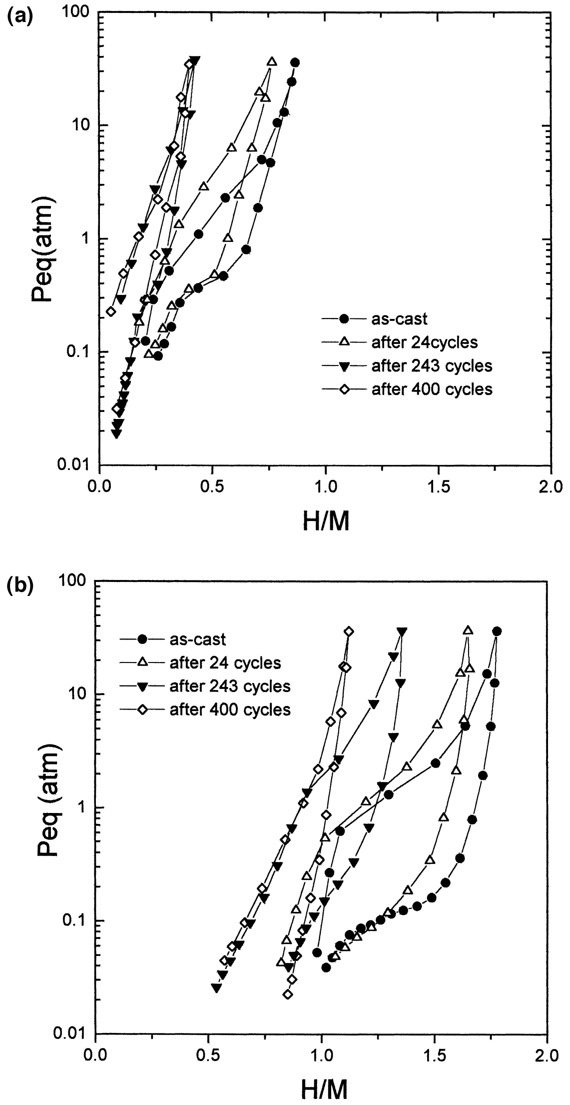

Fig. 2. (a) *P–C* isotherms of sample at 150°C before and after thermal cycling 24, 243, and 400 cycles (temperature=RT~600°C, *P*=10 atm H_2, cycle time=20 min); (b) *P–C* isotherms of sample at 600°C before and after thermal cycling 24, 243, and 400 cycles (temperature=RT~600°C, *P*=10 atm H_2, cycle time=20 min).

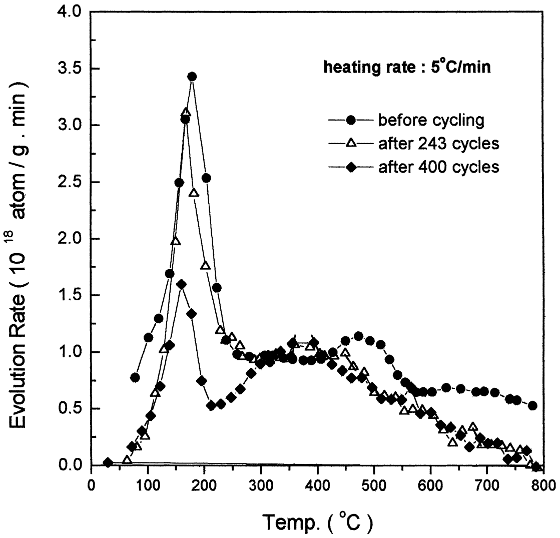

Fig. 3. Thermal desorption spectra of $(V_{0.53}Ti_{0.47})_{0.925}Fe_{0.075}$ hydrides before and after cycling.

from Fig. 2(b) decreases by about 40% after 400 cycles, even gradually with increasing cycle. The hydrogen storage capacity of the high plateau region decreases by about 16% after 400 cycles. To further investigate the degradation behavior thermal desorption analysis was performed on samples before and after thermal cycles (243 and 400 cycles). Fig. 3 shows the results of the thermal desorption of hydrogen from hydrided samples before and after cycling in the thermal desorption spectra. Two peaks appear for each sample. Since the position of peaks is closely related to the interaction energy between hydrogen atoms and occupied sites [15], the two peaks at low and high temperature correspond to the low and high interaction energies respectively, the peaks at the low and high temperature are related to the desorption of hydrogen in high and low plateau regions respectively. The peak area represents the amounts of hydrogen evolved from a specific site [15], therefore the degradation state can be confirmed qualitatively by measuring the change of the integrated peak area. As shown in Fig. 3, two peaks at around 180 and 470°C for the activated sample, two peaks at around 180 and 370°C for the degraded samples after 243 and 400 cycles, respectively. The position of the low temperature peak is not changed but the peak area gradually decreases with increasing cycle number. However the position of the high temperature peak is shifted to a lower temperature region and the peak area decreases mainly during the initial 243 cycles. After that, the peak position and area are not changed much up to the 400th cycle.

To find out the cause of degradation it is necessary to investigate the structure of samples. XRD analysis was performed on the samples in their de-hydrided and hydrided state before and after degradation. Fig. 4 shows the result of XRD analysis before and after thermal cycling for the samples in de-hydrided state. This sample (α phase) before cycling exhibits a homogeneous single phase having a BCC structure. However the degraded sample after 243 cycles exhibits BCT structure. Fig. 5 shows the result of XRD analysis before and after thermal cycling of the samples in their hydrided state. The sample (γ phase) before cycling exhibits a homogeneous single phase FCC structure. The degraded sample after 400 cycles also exhibits an FCC structure, but its XRD peaks are broadened.

On the basis of these results, the thermal desorption spectra (Fig. 3) can be interpreted as follows. The high temperature peak represents hydrogen atoms occupying sites in the α phase. Because the structure changes from BCC to BCT after 243 cycles, i.e. to a less stable phase

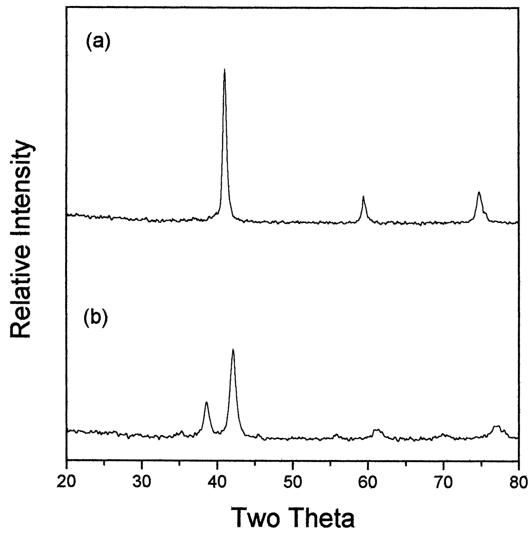

Fig. 4. XRD patterns of samples: (a) activated; and (b) degraded in de-hydrided state.

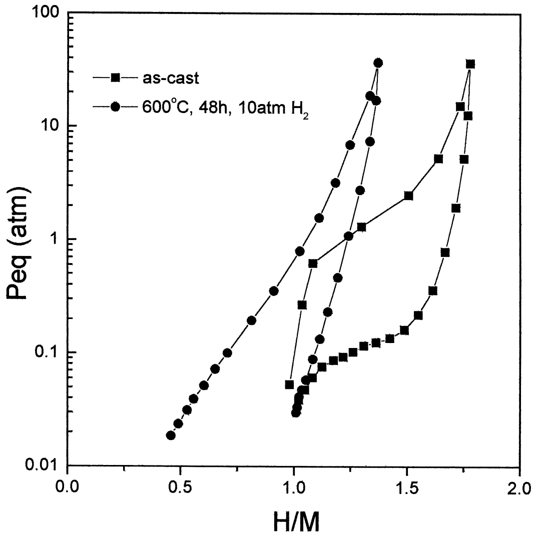

Fig. 6. *P–C* isotherm of sample at 150°C is hydrogenated at 600°C and 10 atm H_2 for 48 h.

with lower capacity, the position of the peak shifts to lower temperature and the peak area decreases mainly after 243 cycles. The lower temperature peak represents hydrogen atoms that occupy the sites in the γ phase. Because the structure is retained as FCC, i.e., the same as the initial hydride of high plateau region, the position of the peak does not shift. The gradual decrease of the peak area and the decrease in the amount of hydrogen can be related to the peak broadening in XRD data.

In general, the intrinsic degradation is greatly affected by the temperature and hydrogen pressure during thermal cycling. When hydrogen is absorbed or desorbed, the lattice volume is expanded and contracted about 20%. Therefore a large elastic strain forms in lattice which can affect the thermodynamic stability of metal hydride. Hydrogenation treatments at elevated temperature induce a loss of reversible hydrogen storage capacity. For example, the hydrogen storage capacity of the $ErFe_2$ crystalline compound decreases drastically depending on the charging temperature and pressure [16]. Summing up, the elastic strain accumulation in the matrix during repetitive cycling and the elevated temperature cause the sample to change into a more stable thermodynamic state. It can be suggested that the intrinsic degradation of $(V_{0.53}Ti_{0.47})_{0.925}Fe_{0.075}$ is motivated by the elastic strain and temperature effects.

In order to investigate the effect of temperature only, a static isothermal hydrogenation treatment at high temperature was performed on the activated sample. With this treatment the effect of elastic strain caused by hydrogen

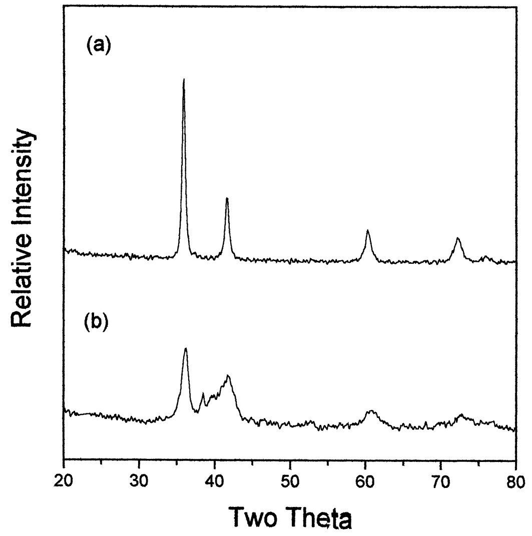

Fig. 5. XRD patterns of samples: (a) activated; and (b) degraded in hydrided state.

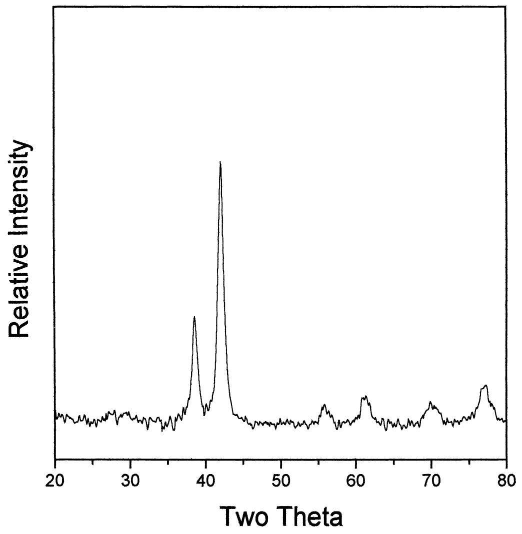

Fig. 7. XRD pattern of sample hydrogenated at 600°C and 10 atm H_2 for 48 h in de-hydrided state.

absorption and desorption can be eliminated. Fig. 6 shows the *P–C–T* curve of a sample hydrogenated at 600°C under a hydrogen charging pressure of 10 atm for 48 h. Under these conditions the absorbed hydrogen capacity of the low plateau region drastically decreases by about 24%. From Fig. 6, it can be inferred that the application of elevated temperature without elastic strain energy causes a large capacity loss in this alloy. To investigate the change of crystal structure after a static isothermal hydrogenation treatment, a sample in a de-hydrided state was prepared and subjected to XRD analysis. Fig. 7 shows that initial BCC structure can change to BCT structure only by temperature effects. This phenomenon is the same after thermal cycling. From these facts, it can be said that the decrease of hydrogen storage capacity of the low plateau region is caused only by the elevated temperature during thermal cycling. However, the reason for the degradation of the high plateau region is still not clear. Since XRD analysis after thermal cycling showed broadened peaks, which may be caused from a disordered structure, TEM analysis was carried out to investigate this phenomenon. Fig. 8 shows the bright field image and its corresponding electron diffraction pattern of the degraded sample after 400 thermal cycles. TEM analysis shows a featureless and mottled structure which is typical of amorphous materials and the broad diffuse halo ring pattern corresponding to an amorphous phase. In many rare-earth based intermetallic compounds it is well known that the hydrogen absorption and desorption cycling induces a transformation of crystalline hydride to an amorphous phase [17–19]. Especially Chung and Lee [17] reported that the La_2Ni_7 intermetallic compound could be amorphized by thermal cycling. It was thereby suggested that the amorphization by thermal cycling was closely related to the lattice distortion caused by repetitive elastic strain accumulation. From these facts it is reasonable to say that the hydrogen storage capacity in the high plateau region decreases with the formation of the amorphous phase in the FCC matrix phase.

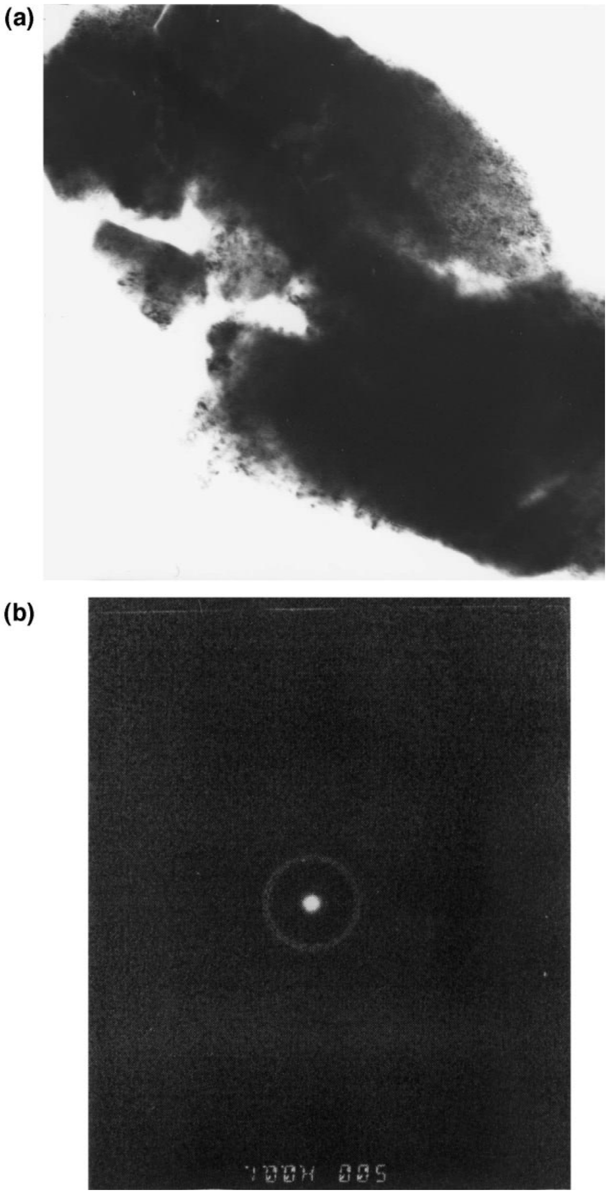

Fig. 8. (a) Bright field TEM image of degraded sample; and (b) corresponding electron diffraction pattern.

4. Conclusions

The $(V_{0.53}Ti_{0.47})_{0.925}Fe_{0.075}$ alloy which has two plateau regions was thermally cycled between room temperature and 600°C under a hydrogen pressure of 10 atm. About 40% of the hydrogen storage capacity was lost after 400 cycles. A BCT phase and an amorphous phase were formed as degradation products. The phase transformation from the BCC to the BCT phase was caused only by the elevated temperature under a hydrogen atmosphere. This phase transformation caused the degradation of the low plateau region. The formation of an amorphous phase within the FCC matrix phase caused the degradation of high plateau region.

Acknowledgements

This work was conducted under the R & D programs on The Development of Clean Starter Using Metal Hydride sponsored by Taedok Institute of Technology and Yukong Industrial Co., Ltd. We wish to express our thanks to the Research Center for Hydrogen Energy, KAIST for financial support for a part of this work.

References

[1] S. Suda, Y. Komazaki, H. Narasaki, M. Uchida, J. Less-Common Met. 172–174 (1991) 1092.

[2] M. Wierce, R. Werner, M. Groll, J. Less-Common Met. 172–174 (1991) 1111.
[3] R. Werner, M. Groll, J. Less-Common Met. 172–174 (1991) 1122.
[4] M. Ron, J. Less-Common Met. 104 (1984) 259.
[5] H. Gjurstorm, Y. Komasaki, S. Suda, J. Less-Common Met. 131 (1987) 1122.
[6] G.H. Kim, J.Y. Lee, J. Less-Common Met. 132 (1987) 123.
[7] H. Ishikawa, K. Oguro, A. Kato, H. Suzuki, E. Ishi, J. Less-Common Met. 120 (1986) 123.
[8] R.L. Cohen, K.W. West, J.H. Wernick, J. Less-Common Met. 95 (1983) 17.
[9] H.J. Ahn, S.M. Lee, J.Y. Lee, J. Less-Common Met. 142 (1983) 253.
[10] S.S. Park, J.Y. Lee, Z. Phys. Chem. N.F. 163 (1989) 1337.
[11] P.D. Goodell, J. Less-Common Met. 99 (1984) 1.
[12] M.J. Benham, D.K. Loss, C. Lartigue, A. Percheron Guegan, Z. Phys. Chem. N.F. 147 (1979) 205.
[13] K. Nomura, J. Alloys and Compounds 231 (1995) 513–517.
[14] J.M. Park, J.Y. Lee, Mater. Res. Bull. 22 (1987) 455.
[15] W.Y. Choo, J.Y. Lee, Metall. Trans. A 13 (A) (1982) 135.
[16] H.J. Ahn, Y.G. Kim, J.Y. Lee, J. Alloys and Compounds 196 (1993) 45.
[17] U.I. Chung, J.Y. Lee, J. Non-Cryst. Solids 110 (1989) 203.
[18] U.I. Chung, J.Y. Lee, Acta Metall. Mater. 38 (1990) 811.
[19] Y.G. Kim, U.I. Chung, J.Y. Lee, Acta Metall. Mater. 40 (1992) 1497.